Nano World Journal

https://doi.org/10.17756/nwj.2024-s1-016

Research Article

Open Access

Synthesis and Characterization of Some Nanoparticle Decorated with a Pyridine Ring and Containing Schiff Bases

Ban D Saleh[1*], Afrah H. Hazaa[2] and Ghazwan H. Abdullwahhab[3]

[1]*Department of Chemistry, College of Education for Women, Tikrit University, Tikrit, Iraq*
[2]*Department of Samarra Education, Directorate of Salah El-din, Ministry of Education, Samarra, Iraq*
[3]*Department of Chemistry, College of Education for Pure Sciences, Tikrit University, Salah Al-Din, Iraq*

[*]Correspondence to:
Ban D Saleh
Department of Chemistry,
College of Education for Women,
Tikrit University,
Tikrit, Iraq.
E-mail: baan.saleh@tu.edu.iq

Received: January 03, 2024
Accepted: March 07, 2024
Published: March 12, 2024

Citation: Saleh BD, Hazaa AH, Abdullwahhab GH. 2024. Synthesis and Characterization of Some Nanoparticle Decorated with a Pyridine Ring and Containing Schiff Bases. *NanoWorld J* 10(S1): S84-S92.

Copyright: © 2024 Saleh et al. This is an Open Access article distributed under the terms of the Creative Commons Attribution 4.0 International License (CCBY) (http://creativecommons.org/licenses/by/4.0/) which permits commercial use, including reproduction, adaptation, and distribution of the article provided the original author and source are credited.

Published by United Scientific Group

Abstract

In this study, a series of nano graphene derivatives incorporating Schiff bases were functionalized and immobilized onto a pyridine ring in a two-step process. Firstly, graphene oxide (GO) was prepared using the Hummer method, followed by the synthesis of nitrogen-doped reduced graphene oxide (NRGO) particles through the reaction of GO with aqueous hydrazine ($NH_2NH_2.H_2O$). The NRGO nanoparticles were further modified by electrically preparing pyridine aromatic derivatives (ArNRGO) on their surface. The carboxyl groups of the graphene plates were subsequently modified by thermally inducing the reaction with thiocarbazide (TCH), derived from a mixture of carbon disulfide, resulting in the formation of ArNRGOTC, which exhibited triazole functionality. Moreover, some derivative of the nanoparticle base, ArNRGOTZS, was synthesized using the refractory compounds method.

Keywords

Schiff base, Nitrogen atoms, Potassium permanganate, Fourier transform infrared spectroscopy, X-ray diffraction, Scanning electron microscopy

Introduction

The nanosheets, which are flat sheets, the thickness of these sheets is the diameter of one carbon atom, and the hybridization process between carbon atoms is in the form of (SP_2). The SP_2 hybridization process means the fusion of orbitals present in two adjacent carbon atoms and bonding between them [1]. Triazoles are heterocyclic aromatic compounds with the molecular formula $C_2H_3N_3$. They were named by this name for the first time by the scientist Potts [2]. Their name includes the unsaturated site 1H and 4H and the number of nitrogen atoms, tri. They are of two types depending on the bonding of the nitrogen atoms in them. First: Identical triazoles, which are compounds in which the nitrogen atoms are not all bonded together, as they are separated by the two carbon atoms and it is present in the form of two isomers due to the presence of the tautomeric state [3, 4]. The equatoriality can be observed in the steric form of the triazoles [5]. Secondly, the triazoles are adjacent to the site, and they are the compounds in which the three nitrogen atoms are connected to each other. Natural graphite is the basic material for the preparation of GO and the most common source of it [6]. The reason is that natural graphite contains many localized defects in its structure that may serve as starting points for chemical reactions [7]. Possible interactions of active aggregates in the composition of graphite can be clarified in the presence of acids and oxidation agents such as (Potassium permanganate, $KMnO_4$) to prepare GO and then NRGO through Hummer's method in which sodium nitrate and oxidizing agents catalyzed by sulfuric acid were mixed with graphite in an aqueous medium [8, 9]. Where sulfuric acid and oxidizing agents

($KMnO_4$) work by penetrating between the layers inside the graphite crystals, and when the temperature is raised, this will lead to the spacing of the layers due to the oxidation that occurs between the layers, so the oxygen atoms will repel, which is caused by the repulsion of the layers partially or completely. Nanomaterials can be classified into several forms, and these forms. They are quantum dots, nanoparticles, nanowires, nanocomposites, nanotubes, fullerenes, and nanoparticles. Graphite is another form of carbon, where each carbon atom is triple bonded with three other carbon atoms within the same spatial plane, so that we eventually get compact rings. Hexagonal, as is the geometric shape in aromatic hydrocarbons [10]. The graphite is multi-layered, its structure is flat, and its atoms are covalently bound by three valence electrons, while the fourth electron remains free, which explains its high conductivity and is linked to each other by van der Waals forces, which makes it easy to separate its layers. Graphite is of interest to nanotechnologists, due to its two important properties: strength and electrical conductivity [11].

Experimentation

Instruments

Electric balance, melting point, ultra sonic water bath, Fourier transform infrared (FTIR) spectroscopy, centrifuge, scanning electron microscopy (SEM), oven, X-ray diffraction (XRD), thermal gravimetric analysis, magnetic stirrer, and thermostatic water bath.

Chemicals used

Potassium permanganate, graphite, sodium nitrate, sodium nitrite, hydrochloric acid (80% hydrazine hydrate, ethanol, hydrogen peroxide, Carbon disulfide, P-Hydroxybenzaldehyde, P-Chlorobenzaldehyde P-Bromobenzaldehyde, P-Nitrobenzaldehyde, P-Methoxybenzaldehyde, 4-Aminopyridine, 1-Amino-2-Naphthol-4-Sulfonic acid, and 1-Naphthyl amine.

Preparation of nanoparticle graphene

The preparation was carried out in two steps, the first step is the preparation of GO (Hummer method), an amount of graphite was added to a mixture of 46 ml of concentrated sulfuric acid and an amount of sodium nitrate gradually for 10 min, an amount of $KMnO_4$ was added to the mixture while maintaining the temperature less than 20 m, It was left to stir magnetically for 2 h, then 46 ml of distilled water was added to the mixture, after which the temperature was raised to (98 °C), then 140 ml of warm distilled water was added, then 15 ml of hydrogen peroxide (30%) was added and left to stir, then Add 300 ml of distilled water and leave the mixture for 24 h, collect and then wash the precipitate and dry it until the weight stabilizes [12]. The second step is to prepare graphene nanoparticles (NRGO), 1 ml of aqueous hydrazine was added to a clear solution of GO and 1 ml of hydrochloric acid, and the mixture was raised at a temperature of 100 °C for 2 h. The formed black precipitate was collected, washed with deionized water, and dried at a temperature of 70 °C [13].

Preparation of TCH

5 ml of carbon disulfide was added gradually over 10 min to (20 ml) of aqueous hydrazine 80%) in a suitable beaker at a temperature of 0 °C with continuous stirring. The reaction mixture was elevated for 30 min, then it was cooled in an ice bath, collected. The precipitate formed (yellow white) by filtration and washing with ethanol, and until the color of the precipitate turned white, it was collected and recrystallized with distilled water, then dried at (70 m^3) until the weight stabilized (Figure 1) [14].

Preparation of the aromatic derivative of nanoplatelets by electrophoresis (ArNRGO)

ArNRGO was prepared in two steps: the first step was the preparation of diazonium salts. (0.282 g of 4-Aminopyridine) was added to a flask containing an acidic solution (1:1 water: concentrated hydrochloric acid 37%) with the temperature fixed within the range 0 - 5 m, and in another beaker, dissolve 0.003 mol x 0.207 g of sodium nitrite in an appropriate amount of distilled water and add to the first solution gradually while keeping the temperature within the range 0 - 5 °C with continuous stirring for a period of 20 - 30 min in a dark atmosphere. It was not diagnozed, but it was used directly in the second step [15]. The second step was the preparation of highly aromatic nanoplatelets. 0.1 g of NRGO, was added to 25 ml of distilled water, and placed in an ultrasound machine until the solution became clear without plankton. The solution was added. The liquid to the electric cell consisting of platinum electrodes connected to a voltage of 1.6 V with continuous stirring, then the solution of the first step was added to it in the form of drops with cooling in an ice bath, the cell remained on continuous stirring for 24 h continuously, washing the solution three times with deionized water and dried at 50 °C (Figure 2) [16].

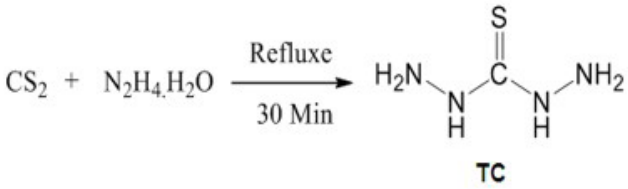


Figure 1: Preparation of TCH.

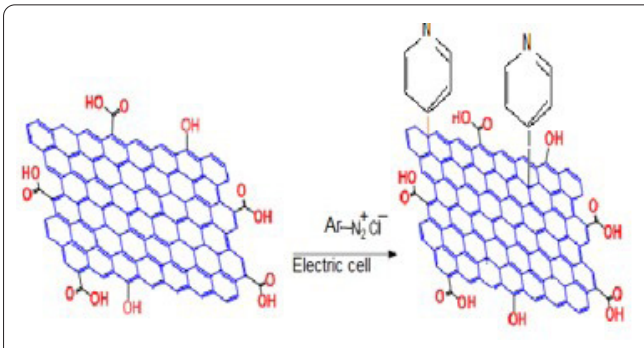


Figure 2: Preparation of ArNRGO.

Preparation of the triazole derivative (ArNRGOTZ)

Mix an amount of ArNRGO with an amount of TCH in a heat-resistant flask, heat the mixture in an oil bath with stirring with a glass stirrer for about five minutes and until the molten changes color and nature, cool the product to room temperature (Figure 3) [17].

Preparation of Schiff nanobases (ArNRGOTZS) compounds (1-3) by thermal melting

Mix 0.1g ArNRGOTZ with 0.3 g of 4-Nitrobnzaldehyde or 0.3 g of 4-Chlorobenzaldehyde or 0.3 g of 4-Methoxybenzaldehyde in a heat resistant flask, heat the mixture in an oil bath while stirring with a glass stirrer for 5 - 10 min at a certain temperature, and when the color of the molten material changes and the nature of its texture, the product is cooled to room temperature (Figure 4) [18].

Results and Discussion

Preparation of GO nanosheets

GO is prepared from the possible reactions of the active groups in the composition of graphite in the presence of acids and oxidizing agents such as ($KMnO_4$) and according to the mechanism shown in figure 5.

Preparation of NRGO nanosheets

NRGO was prepared from the reaction of GO with aqueous hydrazine (80%) ($NH_2NH_2.H_2O$) according to the mechanism shown in figure 6.

Preparation and characterization of ArNRGO

The aromatic nanoplatelets (ArNRGO) were prepared by two steps, the first was the preparation of diazonium salts, and the second was the preparation of a clear solution of NRGO in the electrolysis cell. Infrared, which showed clear values for the stretching of the (OH) group within the range of 3434 cm^{-1}, and clear values for the aromatic ring at the stretching range 1478, 1568 cm^{-1} for the bond (C=C) (Figure 7).

This is evident in the SEM images of the compound ArNRGO, which show the proportion of decoration spaced apart. Despite this, it was found that the undulations are large in the plate. This may be attributed to the presence of additional peeling resulting from the liberation of nitrogen gas with the presence of the basic characteristic of pyridine that leads to the spacing of the layers with repulsion, and this is observed from figure 8e which shows layers up to 8.92 nm and is also supported by the particle size D = 2.5 nm as well as the low number of layers 7 [19] as shown in figure 8.

The compound ArNRGO showed an XRD spectrum that had angle values of 2θ different from NRGO and grafting the aromatic compound onto a plate of NRGO gave values of interfacial distances (0.38, 0.37, 0.34 nm) which differed from the NRGO, whose distance was 0.36 nm, with angle values respectively (25.72˚, 23.75˚, 23.03˚) and an average particle size of 2.54 nm and a number of 7 layers, as shown in figure 9.

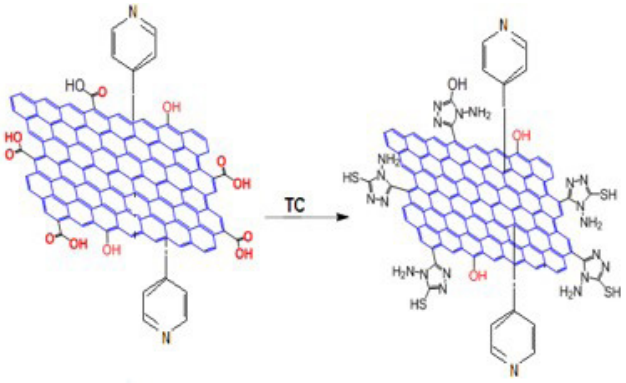


Figure 3: Preparation of ArNRGOTZ.

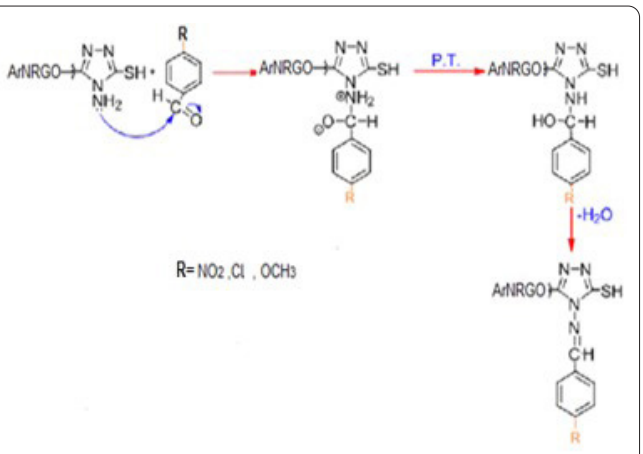


Figure 4: Preparation of ArNRGOTZS.

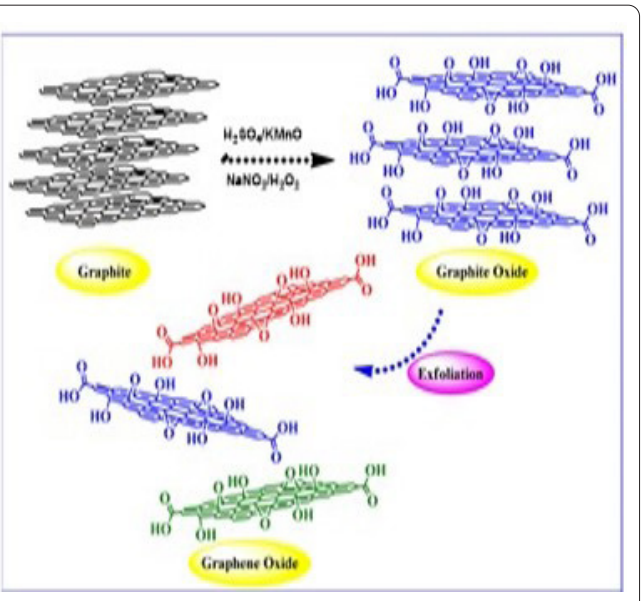


Figure 5: Preparation of GO.

Preparation and characterization of ArNRGOTZ

It was prepared from thermal melting of Ar-NRGO with TCH in an oil bath with stirring at a temperature of 171 ˚C. Until the color and nature of the molten changed, the ArNRGOTZ compound was identified by observing some of its physical properties and by FTIR, which showed its disappear-

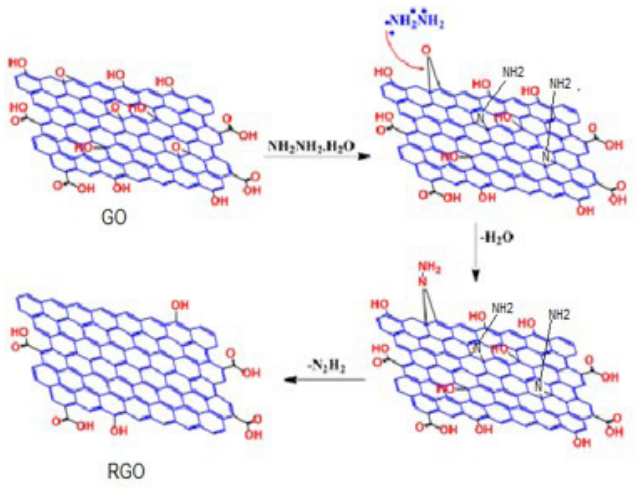


Figure 6: Preparation of NRGO.

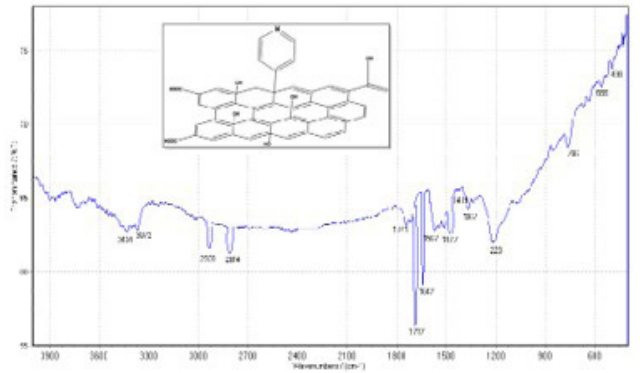


Figure 7: FTIR spectrum of ArNRGO.

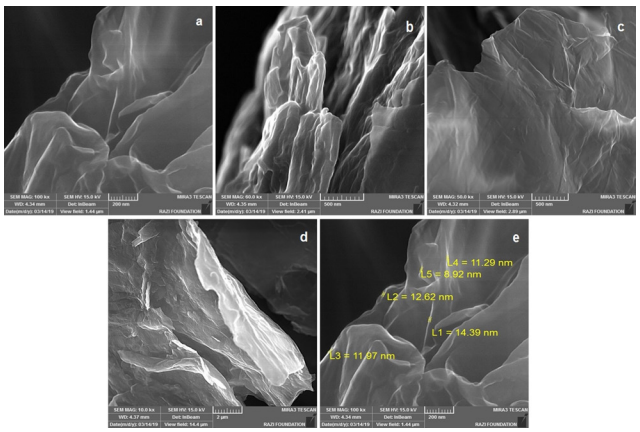


Figure 8: SEM images of ArNRGO.

ance. The carbonyl group (νC=O) within the range of 1717 cm^{-1}, which was evident in the aromatic nanoplates of the ArNRGO compound and showed a broad and distinct clear band due to the stretching of the alcoholic hydroxyl groups on the surface and sides of the triazole plate within the range of 3444 cm^{-1}, in addition to two bands. The symmetrical and asymmetrical stretches of the primary amine group within the ranges 3221, 3256 cm^{-1}, as shown in figure 10.

Figure 11 of the compound ArNRGOTZ using SEM.

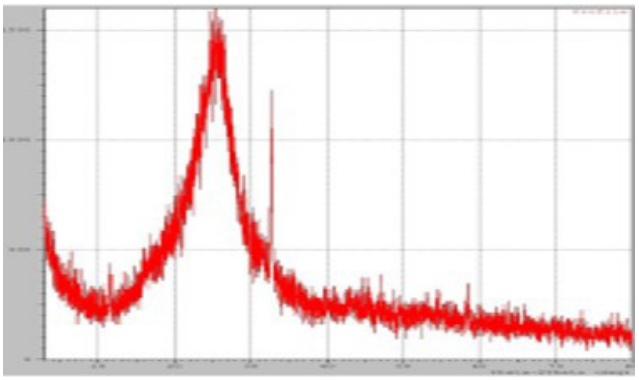


Figure 9: XRD spectra of ArNRGO.

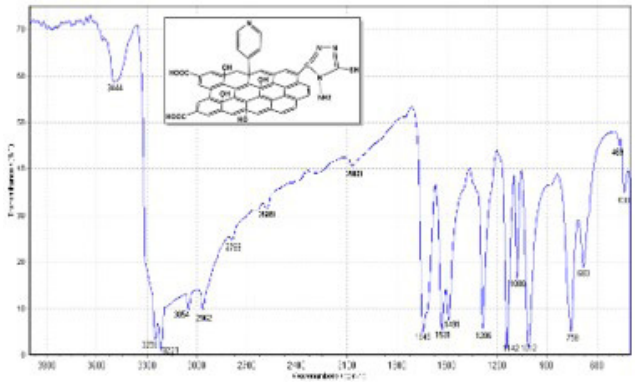


Figure 10: FTIR spectrum of ArNRGOTZ.

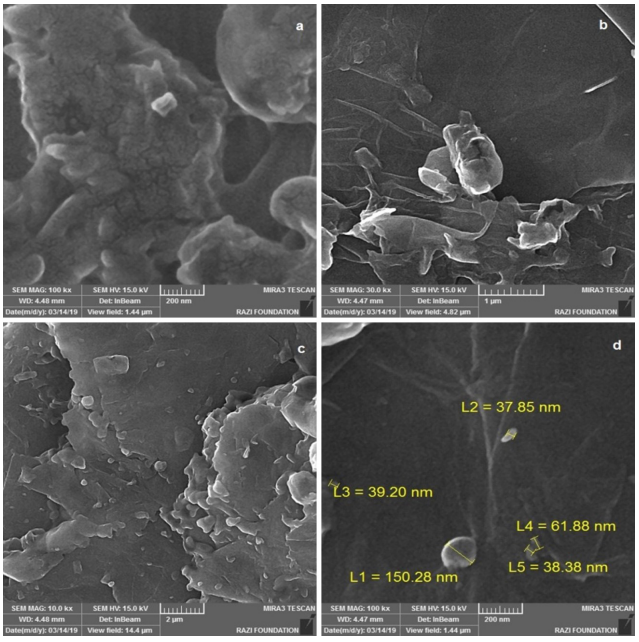


Figure 11: SEM images of ArNRGOTZ.

Figure 11a and 11c show the distribution pattern of the formation of triazole clusters on the edges of the plates with the remainder of the decoration and the presence of clusters on the surface of the plate may be due to the presence of some cracks in it, and the numbers show as in figure 11d the values of the volumes of the clusters that reached 37.8 nm as a min-

imum, with the phenomenon of parallel wrinkles remaining as in figure 11b and in the mother sample ArNRGO with increasing layer clustering up to 134.98 may be attributed to the increased polarization due to the formed triazoles and the possibility of the survival of an amount of TCH between the layers, and this may explain the presence of multiple bands in the XRD spectrum for the sample, figure 12.

XRD measurement of ArNRGOTZ showed angle values of 2θ (28°, 22°, 34°) and interparticle distances 0.31, 0.38, 0.25 nm, respectively, with an average grain size of (34.8 nm) and 134 layers, as shown in figure 12.

Schiff nanobases (ArNRGOTZS) were prepared using the method of thermal melting in the solid phase of the amino substance (ArNRGOTZ) with the used aldehydes, where the reaction took place in 5 - 10 min until the color of the molten changed and the nature of its texture.

Schiff nanobases (Ar-NGTZS1 - 3) (Figure 13, figure 14, and figure 15) were identified by observing some physical properties and FTIR spectroscopy, which showed the disappearance of the primary amine group (NH_2) and the appearance of absorption bands stretching the imine bond (C=N) within the range (1591 cm^{-1}). 1678 cm^{-1} and stretching absorption beams (O-H) within the range (3429 - 3438 cm^{-1}) and showed new absorption beams for structural curvatures type 4,1-compensation for the aromatic ring as well as a stretchy absorption beam (C-Cl) as well as other absorption beams showed notes table 1, figure 16, figure 17, and figure 18.

From the morphological SEM images of the compound (ArNGTZS1), the appearance of twisted filamentous particles is observed at the edges of the stratified clusters (Figure 19c), which have a low bonding density. Figure 19a shows the shapes of the particles in addition to their nanoscale, which reaches 31.16 nm, with a clear spread on the surface, as in figure 19d. These filamentous structures also appear between close lamellae and almost disappear in divergent lamellae. This may be due to the fact that the higher reduction of lamellae is the most divergent, which reduces the chance of formation of triazoles and thus reduces the chance of the formation of Schiff bases and their filamentous 2D structures as in figure 19b, and it can be noted. The particle size from the calculations of the XRD values, which were measured convergently with SEM, was 17.53 nm, with a layer agglomeration of 54.32 (Figure 20).

The SEM images of the compound (ArNGTZS2) (Figure 21) show the presence of bumps that are not present in the original clear structure in the compound of the corresponding triazole (ArNRGOTZ). In movement and therefore expected to be effective in increasing the effective area of the material in the liquid state. The peak of nanoscale measurements up to 32.90 nm is shown in figure 21c with a clear accumulation on the edges as in figure 21a with a bonding between the layers shown by the increase in the granular size compared to the composite (7). Where the sample showed a particle size of 31.2 nm and an accumulated number of layers of 94.7. It is intermediate between the peak of the accumulation of the sample (1), which was equal to 7.36, and the peak of the compound (B), which was 134.8, and this indicates a clear change with the polarization of the plates after each interaction and may indicate an increase in the lateral polarization in the plate that affects the top of the aggregate clearly. specific, not absolute.The SEM of the compound sample ArNGTZS3 shows a strong overlap between the layers through contact with Schiff bases, and this reduced the layer differentiation as in figure 22b and increased the particle size to reach according to the SEM to 107.25 nm as in figure 22d with irregular edges remaining. It does not show any cracks (Figure 22c) and is in the shape of a tentacle as in figure 22a.

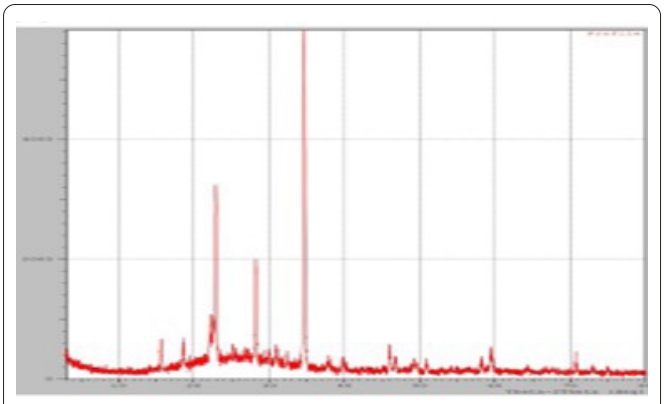


Figure 12: XRD spectra of ArNRGOTZ.

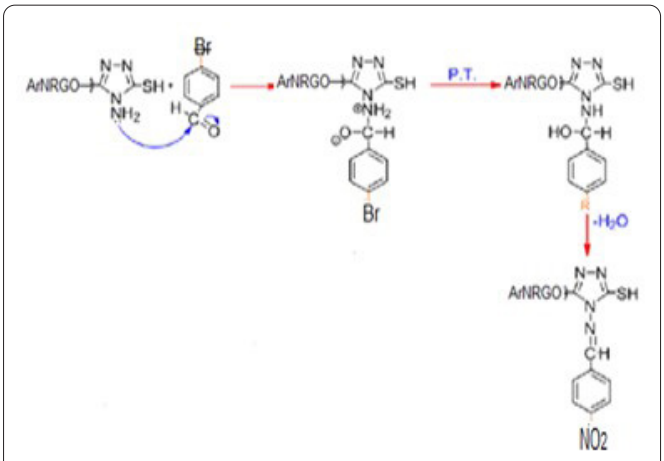


Figure 13: Preparation of Schiff nanoparticles (ArNGTZS1) bases.

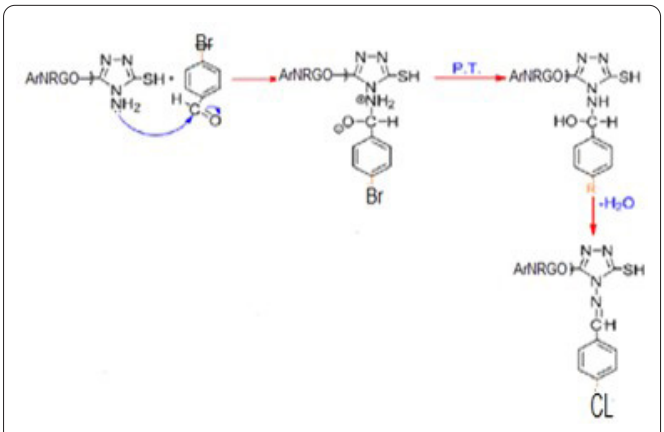


Figure 14: Preparation of Schiff nanoparticles (Ar-NGTZS2) bases.

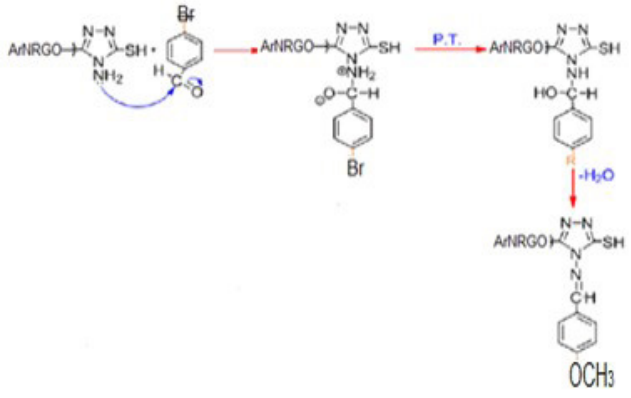


Figure 15: Preparation of Schiff nanoparticles (Ar-NGTZS3) bases.

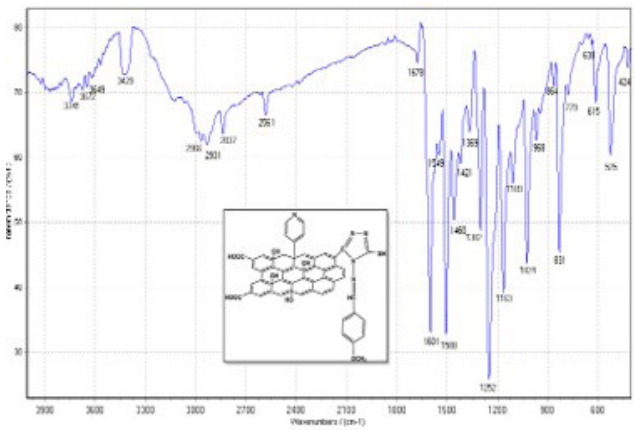


Figure 18: FTIR spectrum of ArNGTZS3.

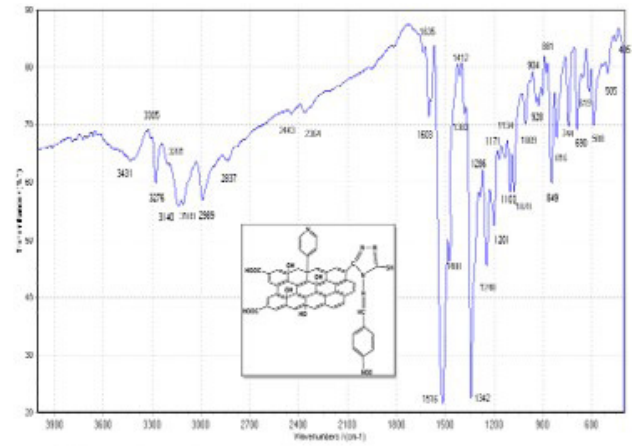


Figure 16: FTIR spectrum of ArNGTZS1.

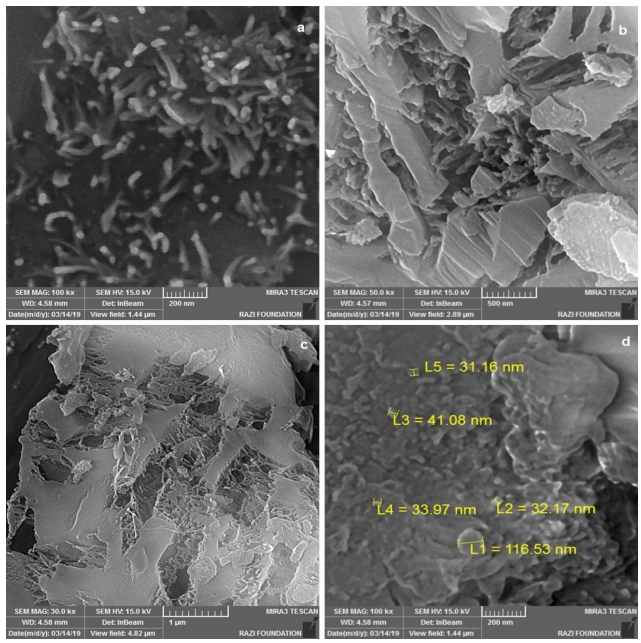


Figure 19: SEM images of compound ArNGTZS1.

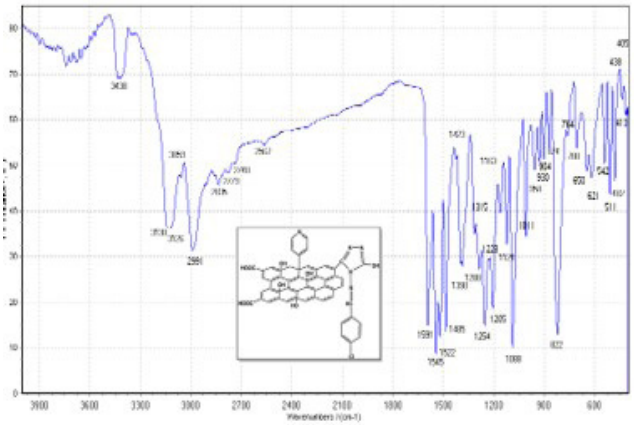


Figure 17: FTIR spectrum of ArNGTZS2.

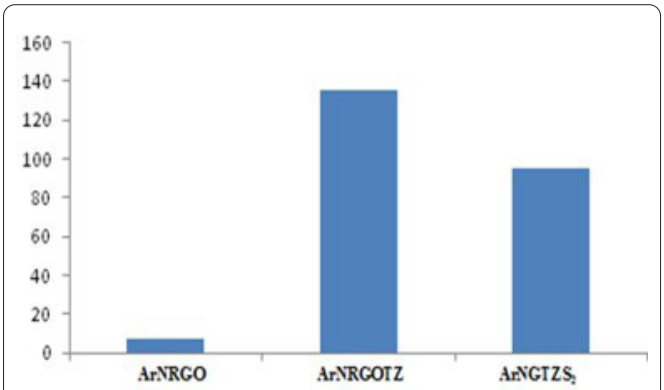


Figure 20: Relationship between compounds (ArNRGO, ArNRGOTZ, and ArNGTZS2) and the number of layers.

The particle size showed an increase in its sequence as planned figure 23 and figure 24 shows the relationship between compounds (ArNRGO, ArNRGOTZ, ArNGTZS3) and the number of layers.

With variation in layer accumulation resulting from the difference in polarization of the plate due to differences in composition. The XRD of the compound (ArNGTZS1) showed angle values of 2θ (20.12˚, 27.6˚, 17.19˚) and inter-particle distances (0.32, 0.44 and 0.51 nm), respectively, with an average grain size of (17.5 nm) and 54 layers, as shown in figure 25.

Table 1: FTIR spectra values for ArNGTZS1 - 3.

Compd. No.	IR ν (cm^{-1})					
	OH	C-H	S-H	C=N	C=Car	Others
1	3431	2989, 2837	2443	1603	1516, 1480	1,4 disub δ C-H arom:849 υNO2: 1516(Overlap),1342
2	3438	2991, 2835	2567	1591	1545, 1485	1,4 disub δ C-H arom:822 υC-Cl: 1088
3	3429	2931, 2837	2561	1678	1545, 1485	1,4 disub δ C-H arom:831 υ C-O-C: 1252,1163

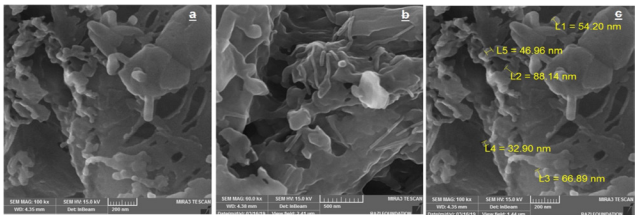


Figure 21: SEM images of compound ArNGTZS2.

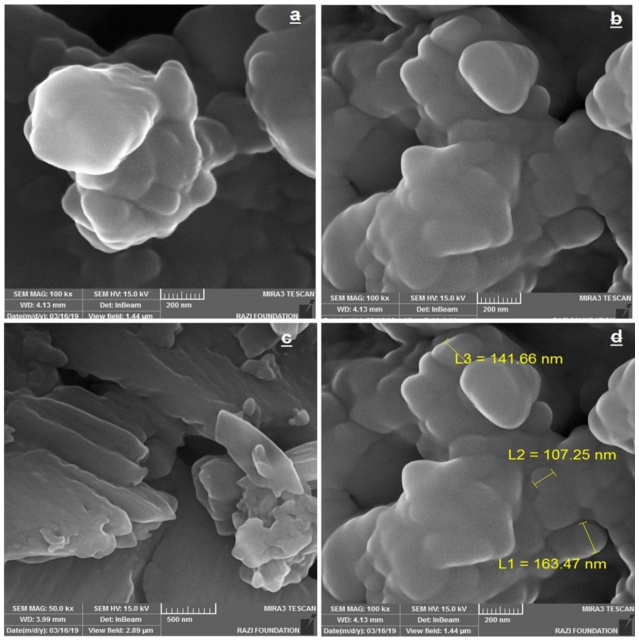


Figure 22: SEM images of compound ArNGTZS3.

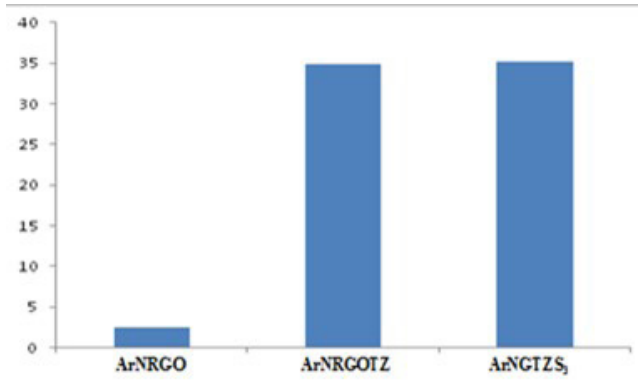


Figure 23: Relationship between compounds (ArNRGO, ArNRGOTZ, and ArNGTZS3) and particle size.

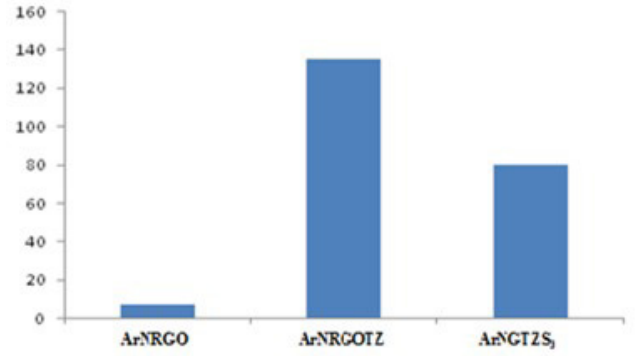


Figure 24: Relationship between compounds (ArNRGO, ArNRGOTZ, and ArNGTZS3) and the number of layers.

The XRD spectra of the compound (ArNGTZS2) showed angle values of 2θ (26.5°, 27.05°, 19.38°), interparticle distance (0.45, 0.33, 0.32 nm), average particle size (31.2 nm), and 94 layers, as shown in figure 26.

The XRD spectra of the compound (ArNGTZS3) showed angle values of 2θ (20.15°, 23.03°, 28.51°), interparticle distances (0.44, 0.38, 0.31 nm), average particle size (35.12 nm) and 79 layers, as shown in figure 27.

From figure 28 it was observed that the relationship between the surface roughness represented by the square root of the average height Sq is directly proportional to the values of the arithmetic heights of the average height in the sample and this indicates that the roughness is represented by the dominant characteristic in the surface. Where the highest value of ArNRGO corresponded to the highest value of ArNGTZS2 and the lowest value of ArNRGOTZ corresponded to the lowest value of ArNGTZS3.

From figure 29 it was observed that most of the samples are of good equatoriality according to the values of kurtosis Sku, except for the ArNRGOTZ sample, which showed high values that clearly indicate the presence of peaks or concavities in a more common form than the equatorial one. Where the lowest kurtosis value was ArNGTZS1, and the highest kurtosis value was ArNRGOTZ.

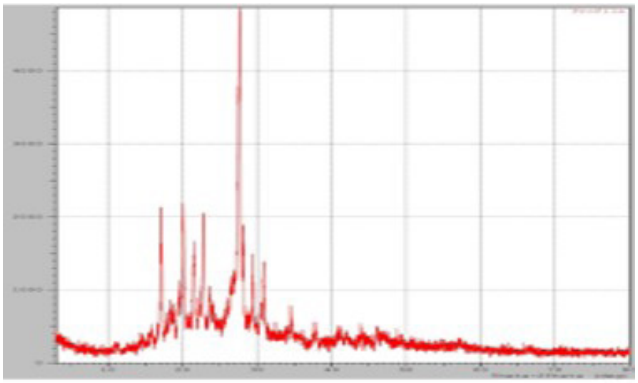


Figure 25: XRD spectra of ArNGTZS1.

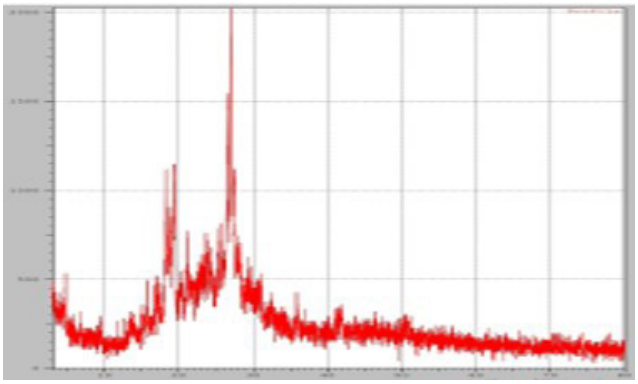


Figure 26: XRD spectra of ArNGTZS2.

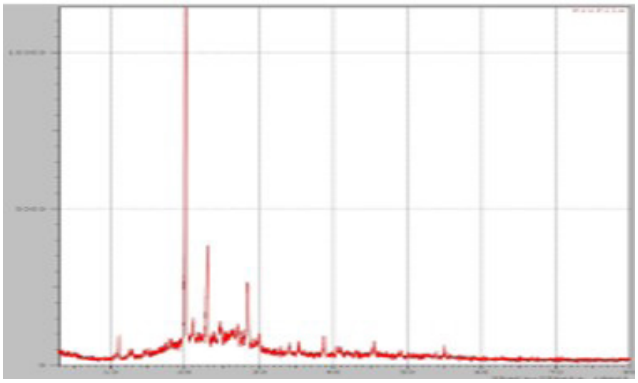


Figure 27: XRD spectra of ArNGTZS3.

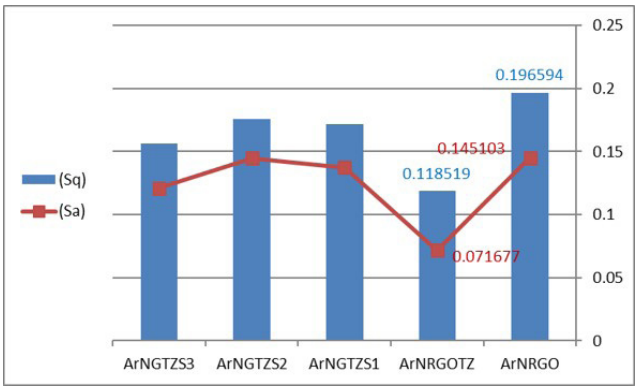


Figure 28: Relationship between the variables Sq and Sa.

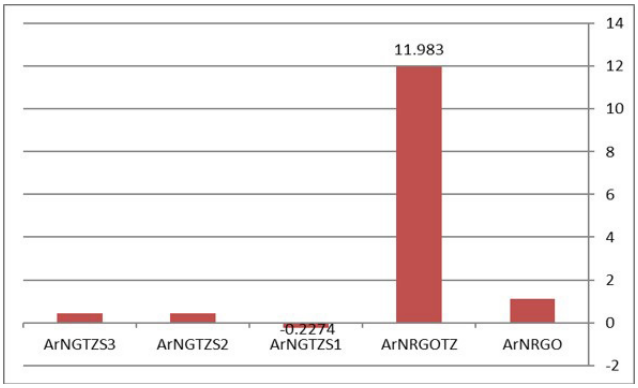


Figure 29: Values of the kurtosis variable (Sku).

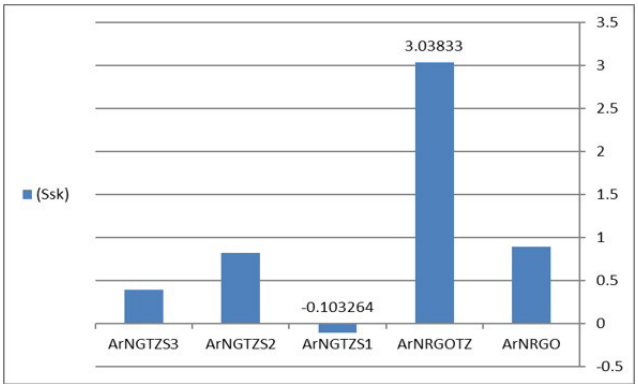


Figure 30: Variable values (Ssk).

From the figure 30 it was noticed that the ArNGTZS1 sample was the only one that showed the value of roughness bias towards the top, while the rest of the samples were all biased to the bottom, i.e., in the form of pits that dominate the number. The ArNRGOTZ triazole sample was also the one with the highest bias value for concavity, which explains the observation in the previous figure that it has the highest value of kurtosis, and this indicates the ability of the distinctive triazole rings to form hydrogen bonds that generate cavities inside the surface.

Conclusion

In conclusion, this research successfully demonstrated the synthesis and modification of GO and NRGO nanoparticles. Through a two-step process, involving the functionalization of graphene derivatives with Schiff bases and subsequent lamination with a pyridine ring, a series of novel nano graphene derivatives were obtained. The introduction of nitrogen-doping and aromatic functionalities onto the graphene surface expanded the potential applications of these materials. The successful modification of carboxyl groups on the graphene plates using TCH further enhanced their chemical versatility. Overall, these findings contribute to the development of advanced graphene-based nanomaterials with tailored properties, holding great promise for various fields including nanoelectronics, catalysis, and sensors. Further investigations can explore the specific applications and performance characteristics of these newly synthesized

graphene derivatives, opening avenues for future research and technological advancements.

Acknowledgments

None.

Conflict of Interest

None.

References

1. Ekimov AI. 1981. Quantum size effect in three-dimensional microscopic semiconductor crystals. *Jetp Lett* 34: 345. https://doi.org/10.1134/S0021364023130040
2. Potts KT. 1961. The chemistry of 1,2,4-triazoles. *Chem Rev* 61(2): 87-127. https://doi.org/10.1021/cr60210a001
3. Bamberger E, De Gruyter P. 1893. On the constitution of cyanophenylhydrazines and the triazole bodies that can be prepared from them. *Rep German Chem Soc* 26(3): 2385-2397. https://doi.org/10.1002/cber.18930260324
4. Papeo G, Pulici M. 2013. Italian chemists' contributions to named reactions in organic synthesis: an historical perspective. *Molecules* 18(9): 10870-10900. https://doi.org/10.3390/molecules180910870
5. Finar IL. 1956. Organic Chemistry: Stereochemistry and the Chemistry Natural Products. Pearson Education India.
6. Krishnan MA, Aneja KS, Shaikh A, Bohm S, Sarkar K, et al. 2018. Graphene-based anticorrosive coatings for copper. *RSC Adv* 8(1): 499-507. https://doi.org/10.1039/c7ra10167h
7. Singu DC, Joseph B, Velmurugan V, Ravuri S, Grace AN. 2018. Combustion synthesis of graphene from wastepaper for high performance supercapacitor electrodes. *Int J Nanosci* 17(2): 1760023. https://doi.org/10.1142/S0219581X17600237
8. Younis TI. 1994. Photometric assay of 1-Naphthylamine by azo coupling. Mosul University. (Graduate Thesis)
9. Wang ML, Liu BL. 2007. Synthesis of 2-mercaptobenzimidazole from the reaction of o-phenylene diamine and carbon disulfide in the presence of potassium hydroxide. *J Chin Inst Chem Eng* 38(2): 161-167. https://doi.org/10.1016/j.jcice.2007.01.003
10. Tolasz J, Vomáčka P, Štengl V, Bludská J. 2015. Photocatalytic composite materials based on graphene and titanium oxide prepared by different methods. In 7th ECCOMAS Thematic Conference on Smart Structures and Materials, Azores, Portugal.
11. Drewniak S, Pustelny T, Muzyka R, Stolarczyk A, Konieczny G. 2015. Investigations of selected physical properties of graphite oxide and thermally exfoliated/reduced graphene oxide in the aspect of their applications in photonic gas sensors. *Photon Lett Pol* 7(2): 47-49.
12. Ahmed JM, Ghazwan AH. 2019. Synthesis and characterization of some new imine grapheme derivatives. College of Education for Pure Science, University of Tikrit. (Graduate Thesis)
13. Li Y, He Y, Xiu J, Wang W, Zhu Y, et al. 2017. Wear and corrosion properties of AISI 420 martensitic stainless steel treated by active screen plasma nitriding. *Surf Coat Technol* 329: 184-192. https://doi.org/10.1016/j.surfcoat.2017.09.021
14. Nalawade A, Nalawade R, Shejwal R, Anuse M. 2017. Synthesis, characterisation, and biological studies of N», N»»-bis [(E)-(4-fluorophenyl) methylidene] thiocarbohidrazide. *Int J Eng Sci Inv* 6(9): 46-49.
15. Brahmayya M, Suen SY, Dai SA. 2018. Sulfonated graphene oxide-catalyzed N-acetylation of amines with acetonitrile under sonication. *J Taiwan Inst Chem Eng* 83: 174-183. https://doi.org/10.1016/j.jtice.2017.12.003
16. Martínez-García G, Agüí L, Yáñez-Sedeño P, Pingarrón JM. 2017. Multiplexed electrochemical immunosensor for obesity-related hormones using grafted graphene-modified electrodes as platforms for antibodies immobilization. *Procedia Technol* 27: 187-189. https://doi.org/10.1016/j.protcy.2017.04.080
17. Rasheed NA, Al-Abdali BI. 2018. Synthesis, characterization and biological activities of 5,5,-(ethane-1, 2-diyl)bis(4-(4-nitrobenzylideneamino)-4H-1,2,4-triazole-3-thio) and its complexes with Cu(II), Cd(II), Hg(II) and Ag(I) ions. *J Global Pharm Technol* 10(03): 417-430.
18. Saleh Al-Jubori HM, Al-salihi KJ. 2021. Synthesis, characterization, and kinetic studies of chelate polymer derived from 3-nonyl benzene and its use for the removal of some heavy metals from aqueous solutions. *Iraqi J Sci* 62(9): 3336-3349. https://doi.org/10.24996/ijs.2021.62.9(SI).4
19. Mohammed YA, Al-Somaidaie GH, Samir AH. Synthesis of carboxylic acid functionalized reduced graphene oxide (RGO) with enhanced heavy metals adsorption capability. *Res J Pharm Biol Chem Sci* 10(3): 1-5.